

Absence of a dissipative quantum phase transition in Josephson junctions: Theory

BY CARLES ALTIMIRAS, DANIEL ESTEVE, ÇAĞLAR GIRIT, HÉLÈNE LE SUEUR, PHILIPPE JOYEZ^a

Université Paris-Saclay, CEA, CNRS, SPEC
91191 Gif-sur-Yvette Cedex, France

a. philippe.joyez@cea.fr

Date: December 22, 2023

Abstract

We obtain the reduced density matrix of a resistively shunted Josephson junction (RSJ), using the stochastic Liouville equation method in imaginary time – an exact numerical scheme based on the Feynman-Vernon influence functional. For all parameters looked at, we find a shunted junction is more superconducting than the same unshunted junction. We find no trace of Schmid’s superconducting-insulating quantum phase transition long believed to occur in the RSJ. This work confirms theoretically a similar conclusion drawn in 2020 by Murani *et al.*, based on experimental observations. We reveal that predictions of an insulating junction in previous works were due to considering Ohmic environments with no UV cutoff.

Table of contents

1 Introduction	1
2 Description of the system	2
3 Evaluating the equilibrium reduced density matrix using path integrals	4
3.1 Numerical implementation	5
4 Results	7
5 Discussion	8
6 Conclusions	11
7 Acknowledgments	12
Appendices	12
Appendix A On the interpretation of Schmid’s QPT in Josephson junctions	12
Appendix B Generation of discrete noise increments with required correlations	13
Appendix C Basis states, operator matrices and thermal expectation values for the bare CPB	14
Appendix D About recent reaffirmations of the existence of Schmid’s dissipative QPT in JJs.	17
Bibliography	17

1 Introduction

In the early 1980’s Caldeira and Leggett [1] introduced a Hamiltonian allowing a rigorous quantum-mechanical description of dissipation in circuits connected to a Josephson junction (JJ). Using this Hamiltonian, they predicted quantitatively how dissipation reduces quantum tunneling of the junction’s phase –a macroscopic electrical variable– and it was precisely confirmed experimentally a few years later [2].

Shortly after Caldeira and Leggett had introduced their modeling of dissipative systems, Schmid [3] showed that a dissipative Quantum phase transition (QPT) should occur for a quantum particle in a 1D periodic potential submitted to friction : Above a well-defined threshold in the friction strength, independent of the potential depth and particle mass, the particle localizes in one well of the potential, while below this threshold it is delocalized, in continuity with the Bloch states that exist in absence of friction.

At the end of his Letter [3], Schmid briefly mentions a resistively shunted Josephson junction (RSJ) is analogous to the system he considers and suggests one could use it as a test bed to observe his predicted *localization* effect. In this analogy, the phase of the junction plays the role of the particle's position, the friction strength scales as R^{-1} , the inverse of the shunt resistance, and Schmid's analogy implies the junction's phase should be localized only when the shunt resistance R is smaller than $R_Q = h/4e^2 \simeq 6.5 \text{ k}\Omega$ and delocalized when $R > R_Q$, irrespective of the junction's characteristics (size, transparency, material...). The standard interpretation of this localization|delocalization dissipative QPT is that at $T = 0$, the JJ should be superconducting for resistances $R < R_Q$ and *insulating* for $R > R_Q$. Even though this predicted insulating phase strangely conflicts with the perturbative limit $R \rightarrow \infty$ and the classical understanding of JJs (see Appendix A), theoretical papers that examined the subject using many different techniques have, to the best of our knowledge, all essentially confirmed this interpretation [4-13] and the phenomenon was linked with quantum impurity problems [14].

In 2020 Murani and co-workers [15] (including some of the present authors) used state-of-the-art experimental techniques to investigate squids shunted with resistances $R \geq 1.2 R_Q$ and observed no sign of a quantum critical behavior [16]: a dc magnetic flux was modulating the measurements (implying the squid loop hosted a dc supercurrent, hence not being insulating), with no T -power-law dependence of the modulation amplitude at low temperatures. Based on these experimental observations, Murani and co-workers concluded to the absence of the insulating state predicted by the standard interpretation of Schmid's analogy for Josephson junctions. Subsequently, a few papers [17-21] explicitly reaffirmed the existence of Schmid's "insulating state" in Josephson junctions, at least in some parameter domain [see Appendix D]. Thus, the scientific community has not yet attained a consensus regarding the presence or absence of Schmid's QPT in JJs. This underscores the current lack of a comprehensive theoretical understanding of the RSJ.

In this work, we bring theoretical support to the conclusion of Murani and co-workers that RSJs are always superconducting in their ground state. To do so, we start from the Caldeira-Leggett description of a junction connected to an arbitrary linear admittance, and use an exact method based on the path integral formalism for obtaining the equilibrium reduced density matrix of the junction and predictions for key observables characterizing the junction's transport properties. Our results show that, for all parameters tested, a resistively shunted Josephson junction is always more superconducting than the same unshunted junction. Our results hence rule out the existence of the predicted QPT. In this process we highlight differences between works predicting the QPT on one side and our present work and experiments on the other side.

2 Description of the system

We model the effect of dissipation on a Josephson junction in the same way as Caldeira and Leggett (CL) [1], with a bath of LC harmonic oscillators providing a linear viscous damping force proportional to the voltage across the junction (i.e. the time derivative of the junction's phase), independently of the value of the phase. The corresponding Hamiltonian is

$$H = E_C N^2 - E_J \cos \varphi + \sum_n 4e^2 \frac{N_n^2}{2C_n} + \varphi_0^2 \frac{(\varphi_n - \varphi)^2}{2L_n}, \quad (1)$$

where $\varphi_0 = \hbar/2e$ is the reduced flux quantum, φ (resp. N) denotes the junction's phase (resp. number of Cooper pairs on the capacitor) which are conjugate and verify $[\varphi, N] = i$, and the φ_n (resp. N_n) denote the phase (resp. dimensionless charge) of the bath harmonic oscillators.

The bath's oscillators are in infinite number, forming a continuum in the frequency domain, characterized by the spectral density of modes

$$I(\omega) = \frac{\pi}{2} \sum_{n=1}^N \omega_n^2 Y_n \delta(\omega - \omega_n) = \omega \operatorname{Re} Y(\omega),$$

where $\omega_n = 1/\sqrt{L_n C_n}$ is the n^{th} mode pulsation, $Y_n = \sqrt{C_n/L_n}$ its admittance, and $Y(\omega)$ the admittance formed by the continuum. Although this model and the numerical technique we employ below can handle any form of the admittance, we will focus here on the so-called Ohmic case where $\operatorname{Re} Y(\omega=0) = 1/R$, with R the dc shunting resistance, such that $I(\omega)$ is linear in frequency at low frequency. For fundamental reasons, any concrete dissipative bath has a UV cutoff frequency [1]. Here, we assume that $\operatorname{Re} Y(\omega)$ has a Lorentzian shape

$$\operatorname{Re} Y(\omega) = \frac{R^{-1}}{1 + (\omega/\omega_c)^2} \quad (2)$$

which would correspond to a LR series circuit, with $\omega_c = R/L$. In a practical implementation of a metallic resistor, the inductance L would be at least de geometrical inductance of the device.

The quadratic forms where the junction's phase appears in the last term of (1) can be expanded, giving

$$H = H_{\text{CPB}} + H_{\text{bath}} + H_{\text{coupling}} + H_{\text{CT}}$$

with the different parts corresponding respectively to the bare Cooper pair box (CPB)

$$H_{\text{CPB}} = E_C N^2 - E_J \cos \varphi,$$

the uncoupled bath of harmonic oscillators

$$H_{\text{bath}} = \sum_n \frac{(2e N_n)^2}{2C_n} + \frac{(\varphi_0 \varphi_n)^2}{2L_n} = \sum_n \hbar \omega_n \left(a_n^\dagger a_n + \frac{1}{2} \right),$$

the coupling term

$$H_{\text{coupling}} = -\varphi_0 \varphi \times \left(\sum_n \varphi_0 \frac{\varphi_n}{L_n} \right) = -\varphi_0 \varphi \times I_Y$$

where the junction phase φ couples to the current I_Y flowing in the admittance $Y(\omega)$, and the so-called counter-term

$$\begin{aligned} H_{\text{CT}} &= (\varphi_0 \varphi)^2 \sum_n \frac{1}{2L_n} \\ &= (\varphi_0 \varphi)^2 \int_0^\infty \frac{d\omega}{\pi} \operatorname{Re} Y(\omega) = \frac{(\varphi_0 \varphi)^2}{2L} \\ &= E_L \varphi^2, \end{aligned}$$

which is essential for having the expected damped equation of motion in the classical limit [1]. Interestingly, the counter-term transforms our CPB Hamiltonian into a fluxonium [22] Hamiltonian at zero external flux

$$H_{\text{CPB}} + H_{\text{CT}} = H_{\text{Fl}}.$$

At this point we already realize that the coupling term scales as $1/R$, making it perturbative in the large R limit. Note that if one considers a fixed cutoff frequency, the counter-term inductive energy E_L also vanishes as $1/R$ (since $1/L = \omega_c/R$). Thus, in this Caldeira-Leggett model, a very large shunt resistor appears as a perturbation to the CPB, in agreement with the intuitive expectation that when R increases to infinity no current can flow into it, so that dissipation disappears and one can just remove the resistance from the circuit. In the case of a purely inductive shunt with $L \rightarrow \infty$, it was shown that one also recovers the physics of a CPB [23] (but we will not appeal to this result in the following).

3 Evaluating the equilibrium reduced density matrix using path integrals

The equilibrium reduced density matrix (RDM) of the CPB (i.e. the junction and its capacitor) at temperature T is obtained as

$$\rho_\beta = \frac{1}{Z} \text{Tr}_b e^{-\beta H}. \quad (3)$$

where $\beta = (k_B T)^{-1}$ is the inverse temperature, $Z = \text{Tr}[\exp(-\beta H)]$ is the partition function of the entire system, and Tr_b corresponds to tracing out the bath oscillators. The matrix elements of the RDM in coordinate representation can be expressed formally in the path integral formalism in imaginary time [1, 24, 25] as

$$\rho_\beta[\phi, \phi'] = \frac{1}{Z} \int \mathcal{D}\varphi \exp\left[-\frac{1}{\hbar}(S_{\text{FI}}^E[\varphi] + \Phi[\varphi])\right], \quad (4)$$

where the functional integral is over all imaginary time paths $\varphi(\tau)$ having the boundaries $\varphi(0) = \phi$ and $\varphi(\hbar\beta) = \phi'$. In this expression, the terms in the exponential respectively denote the Euclidean action of the fluxonium

$$S_{\text{FI}}^E[\varphi] = \int_0^{\hbar\beta} d\tau (E_C \dot{\varphi}^2 - E_J \cos \varphi + E_L \varphi^2), \quad (5)$$

and

$$\Phi[\varphi] = -\frac{1}{2} \int_0^{\hbar\beta} d\tau \int_0^{\hbar\beta} d\tau' \varphi(\tau) K(\tau - \tau') \varphi(\tau'), \quad (6)$$

the Feynman-Vernon influence functional [26], where the kernel $K(\tau) = S_{II}(-i\tau)$ is the equilibrium autocorrelation function of the current in the admittance (shunted at its ends), evaluated for an imaginary time argument. For $t \in \mathbb{R}$, $S_{II}(t)$ is obtained using the quantum fluctuation dissipation theorem and the Wiener-Khinchin theorem

$$S_{II}(t) = 2 \int_{-\infty}^{\infty} \hbar \omega \text{Re} Y(\omega) \frac{e^{-it\omega}}{(1 - e^{-\beta\hbar\omega})} \frac{d\omega}{2\pi} \quad (7)$$

which shows that without a UV cutoff in $\text{Re} Y(\omega)$, $S_{II}(t \in \mathbb{R})$ would be divergent and hence nonphysical. In Eq. (6) this expression is simply prolonged to complex times

$$K(\tau) = S_{II}(-i\tau) = \int_0^{+\infty} \hbar \omega \text{Re} Y(\omega) \frac{2 \cosh\left[\left(\frac{\beta\hbar}{2} - \tau\right)\omega\right] d\omega}{\sinh \frac{\beta\hbar\omega}{2}} \frac{1}{2\pi} \quad (8)$$

and one can check that $\int_0^{\beta\hbar} d\tau K(\tau) = 2E_L$. In Appendix B, we provide analytical expressions for $K(\tau)$, for the Lorentzian $\text{Re} Y(\omega)$ we consider.

For evaluating the path integral (3), we then rewrite the influence functional by means of a Hubbard-Stratonovich transformation. In this process, one introduces an auxiliary random scalar field $\xi(\tau)$ having Gaussian fluctuations verifying

$$\langle \xi(\tau) \xi(\tau') \rangle = S_{II}(-i(\tau - \tau')), \quad (9)$$

such that the double integral in Eq. (6) involving φ at two different imaginary times can be replaced by a single integral involving φ at only one time, averaged over all possible realizations of ξ [27-29]. Upon this transformation Eq. (3) becomes

$$\begin{aligned} \rho_\beta[\phi, \phi'] &= \frac{1}{Z} \int \mathcal{D}\xi W[\xi] \int \mathcal{D}\varphi \exp\left[-S_{\text{FI}}^E[\varphi] - \frac{1}{\hbar} \int_0^{\hbar\beta} d\tau \xi(\tau) \varphi_0 \varphi\right] \\ &= \frac{1}{Z} \int \mathcal{D}\xi W[\xi] \int \mathcal{D}\varphi \exp\left[-\frac{1}{\hbar} \int_0^{\hbar\beta} d\tau (H_{\text{FI}} + \xi(\tau) \varphi_0 \varphi)\right]. \end{aligned} \quad (10)$$

with a Gaussian weight functional $W[\xi]$ ensuring Eq.(9). In the last expression, the rightmost integral corresponds to the Euclidean action of a fictitious fluxonium coupled to a given realization of a random “current noise” $\xi(\tau)$ due to the bath. For any given realization of $\xi(\tau)$, the integral of this action over all φ paths can thus be seen as an element $\rho_\xi[\phi, \phi']$ of a (non-normalized) RDM obeying the imaginary-time stochastic Liouville equation

$$-\hbar \frac{\partial}{\partial \tau} \rho_\xi = (H_{\text{F1}} + \xi(\tau) \varphi_0 \varphi) \rho_\xi \quad (11)$$

of the fictitious fluxonium coupled to the noise source $\xi(\tau)$, so that (10) reads

$$\rho_\beta[\phi, \phi'] = \frac{1}{Z} \int \mathcal{D}\xi W[\xi] \rho_\xi[\phi, \phi'].$$

The later equation translates into a path integral equation for the RDM operators, independently of any choice of basis

$$\rho_\beta = \frac{1}{Z} \int \mathcal{D}\xi W[\xi] \rho_\xi. \quad (12)$$

For obtaining the physical equilibrium RDM of the CPB one then needs to perform the remaining path integral over ξ in Eq. (12). This can be done using the following scheme. For a given realization of $\xi(\tau)$, one starts with $\rho_\xi(\tau=0)$ an equipartitioned diagonal matrix (corresponding to an infinite temperature state of the fictitious fluxonium, appropriate for $\tau=0$) and integrates (11) up to $\rho_\xi(\tau=\hbar\beta)$. This yields a non-normalized RDM matrix with no particular physical meaning. Repeating this numerical integration for a suitable number of drawings of the random noise obeying Eq. (9) amounts to sampling $W[\xi]$, and the normalized average of the different $\rho_\xi(\hbar\beta)$ is expected to converge to the physical equilibrium RDM

$$\frac{\sum \rho_\xi(\hbar\beta)}{\text{Tr} \sum \rho_\xi(\hbar\beta)} \rightarrow \rho_\beta. \quad (13)$$

We stress that if this stochastic averaging converges properly, the resulting density matrix is exact; it takes into account the interaction of the system and the bath to all orders with no approximation. Let us note also that the above path integral method does not actually make any assumption on the system Hamiltonian, and only assumes the bath is linear; it can thus be applied to any open system at equilibrium; it can also be extended to cases where the bath couples to the system through a non-linear function of the system’s coordinate [28]. It can even be extended to real-time out-of-equilibrium dynamics of the system [28, 29] at the price of introducing additional complex cross-correlated real-time stochastic variables.

3.1 Numerical implementation

For the numerical implementation of the above stochastic method, we choose as working basis the K lowest eigenstates states $\{|\Psi_k\rangle, 0 \leq k \leq K-1\}$ of the uncoupled fluxonium. For obtaining these eigenstates, we use an intermediate discretized phase basis $\{\varphi_j = j\delta\varphi, \delta\varphi \ll 2\pi, j \in \mathbb{Z}, |j| < \varphi_{\text{max}}/\delta\varphi\}$, with $N^2 = -\partial^2/\partial\varphi^2$ approximated as a finite difference, so that the Hamiltonian is a tridiagonal matrix in this discretized phase basis. Optimized diagonalization routines yield the first a few hundred eigenstates of such tridiagonal matrices very fast, even when $\pm\varphi_{\text{max}}$ spans many wells of the cosine (low E_L).

Note that our working basis is *very* different from that of the bare CPB which is the reference system we are interested in; this fluxonium basis has notably a much greater densities of levels [23]. At low temperature, the most relevant energy scale for the bare CPB is its transition energy from the ground state to the first excited state $\hbar\omega_{01} = E_1 - E_0$ at zero offset charge (see Appendix C), which varies from $\hbar\omega_{01} \simeq E_C$ when $E_C \gg E_J$ to $\hbar\omega_{01} \simeq \sqrt{E_J E_C}$ in the opposite limit $E_J \gg E_C$. This is the “natural” energy scale we consider in the following, not the transition frequencies of the fluxonium. We choose the truncation of the working basis to encompass all the energy scales we take into account (and φ_{max} in the intermediate basis is set accordingly).

Then, in the working basis, the stochastic differential Liouville equation (11) is numerically integrated using discrete imaginary times steps $\{\tau_m = m\delta\tau\}$, with $\delta\tau = \hbar\beta/M$ and $0 \leq m \leq M-1$, and starting with $\rho(\tau=0) = I_K/K$, with I_K the identity matrix. The actual approximate integration of (11) is performed using the symmetric Trotter iteration scheme

$$\rho_\xi(\tau_{m+1}) = \exp\left(\varphi_0\varphi\xi(\tau_m)\frac{\delta\tau}{2\hbar}\right).\exp\left(-H_{F1}\frac{\delta\tau}{\hbar}\right).\exp\left(\varphi_0\varphi\xi(\tau_m)\frac{\delta\tau}{2\hbar}\right).\rho_\xi(\tau_m) \quad (14)$$

that preserves the positivity of the RDM at each step [30]. In Appendix B, we explain how we generate the random noises $\xi(\tau_m)\delta\tau$ entering this iteration scheme.

As explained above, after numerically integrating Eq. (11) for P different realizations of ξ , we take the average RDM as

$$\bar{\rho} = \frac{\sum_{p=1}^P \rho_{\xi_p}(\hbar\beta)}{\text{Tr} \sum_{p=1}^P \rho_{\xi_p}(\hbar\beta)}. \quad (15)$$

In the large P limit this averaged RDM is expected to tend to the true equilibrium RDM, which must be Hermitian and positive-semidefinite. After a finite number of drawing, $\bar{\rho}$ is not perfectly Hermitian-symmetric, however, it is legitimate to symmetrize it. Indeed, for the problem we consider and in the basis we use, for a given drawing of the $\{\xi(\tau_m)\}$ yielding ρ_ξ , drawing the reversed sequence $\{\xi(\tau_{M-1-m})\}$ is equally probable and would yield the transposed of ρ_ξ (in our working basis, all the matrices in (14) are real). Hence, for each drawing we may just add ρ_ξ and its transposed matrix to our stochastic average, so that it always remain Hermitian symmetric and positive-semidefinite (up to numerical accuracy). When the average has converged sufficiently, symmetrizing or not the RDM does not perceptibly change the expectation values of the observables we consider below.

While obtaining the RDM we can simultaneously evaluate expectation values of any operator A , as

$$\langle A \rangle = \text{Tr} \bar{\rho} A = \frac{\sum w_p \text{Tr} \hat{\rho}_p A}{\sum w_p} = \frac{\sum w_p a_p}{\sum w_p}$$

where $w_p = \text{Tr} \rho_{\xi_p}(\hbar\beta)$, $\hat{\rho}_p = \rho_{\xi_p}(\hbar\beta)/w_p$ is the normalized RDM resulting from the integration of Eq. (11) with the p^{th} noise realization and $a_p = \text{Tr} \hat{\rho}_p A$ the corresponding (nonphysical) expectation value of A . In this expression, the trace of the $\rho_{\xi_p}(\hbar\beta)$ hence appear as the weight of a given noise realization in the final estimate of any expectation value (drawings with large traces correspond to paths with lower action in the path integral). The error bars on the estimated expectation value are obtained from the estimator of the variance of the weighed average using the Central Limit Theorem and the effective number of data points $P_{\text{eff}}(P) = (\sum w_p)^2 / \sum w_p^2$.

At large shunt resistance values and high temperature, the $\{w_p\}$ are such that the effective number of samples $P_{\text{eff}}(P)$ grows fast with the number of drawings P and the weighed means converge well. However, when reducing R , (i.e. increasing the coupling to the bath) at fixed $E_C, E_J, \hbar\omega_c$ and kT , one must increase the number of time steps needed to keep the random increments $\xi(\tau_m)d\tau$ small enough, but after the random walk integration of Eq. (11) this nevertheless translates into an increased variance of the $\{w_p\}$, and a corresponding reduction of P_{eff} . At some point in this increase, the weighed estimation of the expectation values becomes dominated by the few drawings that fall in the (positive side) tail of the w_p distribution, and eventually, the single largest one when $P_{\text{eff}} \simeq 1$ and no longer grows substantially with P . In other words, when R is reduced much, the average is dominated by very few drawings. This indicates that, in this case, the action has a deep and sharp minimum representing only an extremely small volume in the phase space of the ξ noise, making the method extremely inefficient. In such case, whether or not the method can still yield reliable estimates of observables depends on the derivatives of those observables around this minimum. Similarly, when reducing the temperature (all other parameters kept fixed), the number

M of steps in τ also needs to be scaled up, eventually causing the same poor statistics. The R and T ranges where the statistics are poor depend on the other system parameters, and notably on the cutoff frequency. The data presented below are all in regimes where the estimators have small error bars, away from these problematic limits.

4 Results

In Fig. 1 we show the expectation values of rms charge fluctuation $\sigma_N = \langle N^2 \rangle^{1/2}$ and the effective Josephson coupling $\langle \cos \varphi \rangle$ as a function of the reduced temperature $kT/\hbar\omega_{01}$, for different values of E_J/E_C , for the RSJ at large values of R/R_Q . Non-zero values of these expectation values in the ground state attest the junction lets (super)current flow through it. Indeed, $E_J \langle \cos \varphi \rangle$ is the effective Josephson coupling that quantifies the ability of the junction to transport supercurrent; it is also proportional to the inverse of the JJ's effective inductance which would vanish (the inductance would diverge) if the junction were to become insulating. As well, the fluctuations σ_N in the number of transmitted charges would be zero in an insulator. We compare our numerical results for these observables to those obtained for the thermal averages in the bare CPB considering all gate charge values (see Appendix C). For these large resistances, most of the numerical expectation values for the RSJ are found close to that of the CPB. At low temperatures they are found slightly above those of the CPB, but by increasing further the resistance (data not shown) one recovers more closely the bare CPB results, as expected for a vanishing perturbation. At large temperatures some results for σ_N are slightly below the bare CPB values, which we attribute to our basis truncation.

In Fig. 2 we consider the R -dependence of the same expectation values for different ratios E_J/E_C and at the low temperature $kT = 0.01\hbar\omega_{01}$. We observe that both $\langle \cos \varphi \rangle$ and σ_N smoothly increase when R is reduced. In Fig. 3, we show that for large resistance values and at the same low temperature $kT = 0.01\hbar\omega_{01}$, changing the cutoff frequency ω_c of the environment admittance has a weak effect when $\omega_c \lesssim \omega_{01}$, while at large ω_c the expectation values of the RSJ do depend on the actual value of the bath cutoff, the junction becoming more superconducting as ω_c increases.

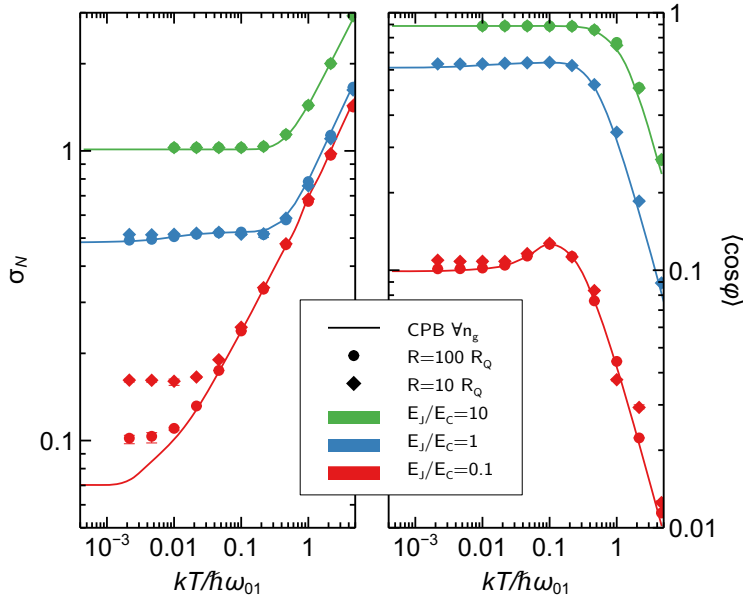


Figure 1. Temperature dependence of the rms charge fluctuations σ_N through the junction (left panel) and the Josephson coherence factor $\langle \cos \varphi \rangle$ (right panel) for large shunt resistor values and different E_J/E_C ratios, for $\hbar\omega_c = 0.4\hbar\omega_{01}$. The thin lines are the thermal expectation values for the unshunted CPB allowing any gate charge (See Appendix C). For these large resistance values, the calculated expectation values (markers) are getting close to the bare CPB values. At low temperature they are found above the bare CPB values, showing that the RSJ is *more* superconducting than in the bare CPB.

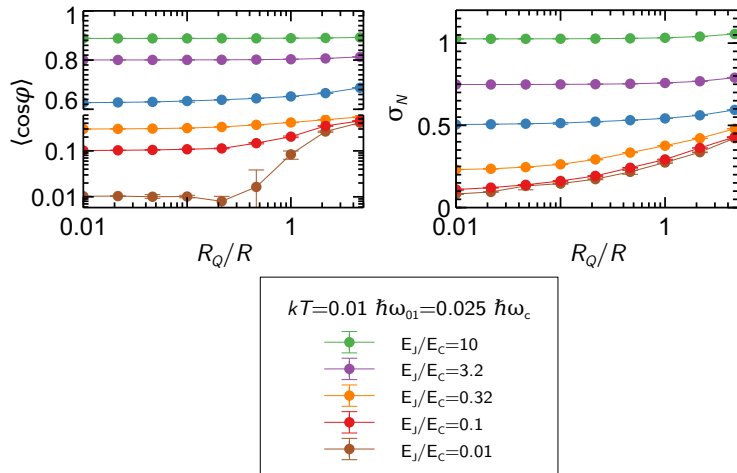


Figure 2. Resistance dependence of the Josephson coherence factor $\langle \cos \varphi \rangle$ (top left panel - note the log-linear broken vertical axis) and charge fluctuations through the junction (top right panel) for different E_J/E_C ratios at the low temperature $kT = 0.01 \hbar\omega_{01}$ and for $\hbar\omega_c = 0.4 \hbar\omega_{01}$. One observes that both $\langle \cos \varphi \rangle$ and σ_N increase when reducing the value of the shunt resistance and tend to saturate at the bare CPB value at large R . No change of behavior is observed around $R = R_Q$.

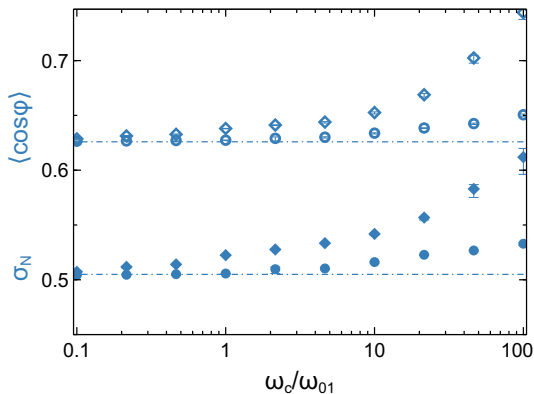


Figure 3. The symbols show the dependence of the Josephson coherence $\langle \cos \varphi \rangle$ (hollow symbols) and charge fluctuations σ_N (filled symbols) expectation values when changing the cutoff frequency ω_c of the environment admittance, for fixed values $R = 100 R_Q$ (circles) or $R = 10 R_Q$ (diamonds), $E_J = E_C$ and $kT = 0.01 \hbar\omega_{01}$. The dash-dotted lines are the corresponding expectation values for the bare CPB at that temperature. At large ω_c , the superconducting properties of the junction increase with ω_c .

5 Discussion

Our numerical results show that the $R \rightarrow \infty$ limit of the RSJ smoothly recovers the well known physics of the CPB family of Josephson qubits, as expected for a vanishing perturbation. In addition, we observe that in the RSJ with a finite shunt resistance, at low temperatures, both the effective Josephson coupling $E_J \langle \cos \varphi \rangle$ and the rms charge fluctuations through the junction σ_N always saturate to values larger (\geq) than in the bare CPB, for all the parameters we tested. This establishes that, in the Caldeira and Leggett model with an Ohmic environment having a finite UV cutoff frequency, the shunted Josephson junction's ground state is *more superconducting* than the bare CPB junction.

These findings can be explained qualitatively by arguing that connecting a resistor to a CPB can significantly affect the ground state of this nonlinear oscillator only if the environment impedance

$Z(\omega) = Y^{-1}(\omega)$ is comparable or lower than the effective impedance of the unshunted CPB at its plasma frequency, such that it can reduce the phase fluctuations across the junction. If furthermore the phase fluctuations of the bare CPB are initially large ($E_C \ll E_J$) the reduction of the phase fluctuations due to the resistor leads to an increase of $\langle \cos \varphi \rangle$, reducing the junction's effective inductance $L_J^{\text{eff}} = (\varphi_0^2) / E_J \langle \cos \varphi \rangle$, and hence its effective impedance, which in turn bootstraps the reduction of the phase fluctuations. Here, the method yields the exact self-consistent solution for these environment-modified fluctuations, similar to Ref. [31], but not restricted to Gaussian fluctuations only. The linear impedance of the bare CPB can be estimated using

$$\frac{Z_{\text{CPB}}}{R_Q} \sim \frac{1}{2\pi} \sqrt{\frac{\langle \varphi^2 \rangle}{\langle N^2 \rangle}}$$

which would be exact for the harmonic oscillator, or as

$$\frac{Z_{\text{CPB}}}{R_Q} \sim \frac{1}{R_Q} \sqrt{\frac{L_{\text{eff}}}{C}} = \frac{1}{2\pi} \sqrt{\frac{2E_C}{E_J \langle \cos \varphi \rangle}}$$

both of which evolving from $\frac{1}{2\pi} \sqrt{\frac{2E_C}{E_J}} < 1$ when $E_C \ll E_J$ to $\propto \frac{E_C}{E_J} \gg 1$ when $E_C \gg E_J$. This roughly explains at which resistance value the upturn of $\langle \cos \varphi \rangle$ occurs in Fig. 2. Yet, for $E_J / E_C \ll 1$, resistances much larger than the above estimates of the CPB linear impedance already induce a substantial change of σ_N compared to the bare CPB.

The temperature dependence of $\langle \cos \varphi \rangle$ is strikingly non-monotonous for large E_C / E_J ratio (see Fig. 1). Starting from low temperatures, it first shows a plateau corresponding to the zero point fluctuations, followed by an increase with a local maximum around $kT / \hbar\omega_{01} = 0.1$, before reducing and finally vanishing at high temperatures. In the experimental results of Ref. [15], a similar non-monotonous variation of the junction's admittance was observed. We believe the remarkable similarity of these features between the experimental data and our numerical simulations constitute a crossed consistency check of the experiment and of the present theoretical approach. Although this effect is easily explained by the resistor allowing charge fluctuations on the capacitor (see Appendix C), to the best of our knowledge, no other theoretical work on the RSJ predicts such behavior.

Our present numerical results show no sign whatsoever of the junction becoming insulating for resistances values larger than R_Q , as predicted in the standard interpretation of Schmid dissipative QPT in JJs. In particular, we observe no change of behavior at or near $R = R_Q$. As well, equilibrium observables related to transport do not follow power laws of the temperature in the critical region of the expected QPT, which would be the numerical signature of that QPT [16]. Hence, in our approach which makes no approximation, the Schmid QPT does not occur in the RSJ. This conclusion brings theoretical support to that of Ref. [15], based on experimental observations.

The results presented here radically differ and contradict the results of all other theoretical works we know which addressed the possible dissipative QPT of the RSJ. These works essentially confirmed the prediction of a superconducting to insulating QPT in JJs, with the effective Josephson coupling renormalized to zero in the insulating phase at $T = 0$, and the JJ phase fully delocalized, with perhaps variants on the precise location of the phase boundary. In the following we specifically discuss the work of Werner and Troyer (WT) [12] who used Quantum Monte Carlo simulations (an exact numerical method in principle equivalent to ours), and whose numerical results show T -power laws of the quantum critical regime, finding the phase boundary at $R = R_Q$, independently of E_J / E_C . The fact that our results (agreeing with experiments and intuitive perturbative limits; no insulating state) differ from those of WT (predicting an insulating state, agreeing neither with perturbative limits nor experiments) points to some key difference between our work and theirs that we now elucidate.

The total action for the system with the bath influence functional we consider, before performing the Hubbard-Stratonovich transformation, is (Eq. (5) and (6))

$$S_{\text{FI}}^E[\varphi] + \Phi[\varphi] = \int_0^{\hbar\beta} d\tau (E_C \dot{\varphi}^2 - E_J \cos \varphi + E_L \varphi^2) - \frac{1}{2} \int_0^{\hbar\beta} d\tau \int_0^{\hbar\beta} d\tau' \varphi(\tau) K(\tau - \tau') \varphi(\tau'),$$

with the kernel K given by Eqs. (8) and (18), while that considered by WT (who cite the review Ref. [13] for it), is

$$S_{\text{WT}}[\varphi] = \int_0^{\hbar\beta} d\tau (E_C \dot{\varphi}^2 - E_J \cos \varphi) + \frac{1}{4} \int_0^{\hbar\beta} d\tau \int_0^{\hbar\beta} d\tau' K(\tau - \tau') (\varphi(\tau') - \varphi(\tau))^2 \quad (16)$$

where the first integral is the action of the Cooper pair box (with no counter-term) and where the kernel $K(\tau)$ has the form

$$K(\tau) = \frac{\pi \hbar}{R (\hbar \beta)^2 \left(\sin \frac{\pi \tau}{\hbar \beta} \right)^2}, \quad (17)$$

corresponding to evaluating Eq. (8) with a purely Ohmic admittance $\text{Re} Y(\omega) = 1/R$, without any UV cutoff. If we ignore for the moment the specific form of their kernel, we can expand the square of phase difference in the influence functional of WT. Then, using the facts that K is even and periodic and that $\int_0^{\beta\hbar} d\tau K(\tau) = 2E_L$, one indeed formally recovers our form of the action with the counter-term,

$$\begin{aligned} \frac{1}{4} \int_0^{\beta\hbar} d\tau \int_0^{\beta\hbar} d\tau' K(\tau - \tau') (\varphi(\tau') - \varphi(\tau))^2 &= \int_0^{\beta\hbar} d\tau E_L \varphi(\tau)^2 \\ &\quad - \frac{1}{2} \int_0^{\hbar\beta} d\tau \int_0^{\hbar\beta} d\tau' \varphi(\tau) K(\tau - \tau') \varphi(\tau'). \end{aligned}$$

We are hence describing the physics of the RSJ on the same grounds, the only difference being the specific form of the kernel $K(\tau)$ we each consider, and which entirely explains the difference between our results, as we now detail.

For the purely Ohmic case WT consider, the τ^{-2} divergence of K at short times in Eq. (17) imposes that the speed (in imaginary time) of the phase on any trajectory remains small and it also kills trajectories that start and end in different wells of the cosine potential. On the other hand, when considering admittances with a UV cutoff, such as we do, influence kernels are more regular at $\tau \sim 0$. For the Lorentzian cutoff (2) we consider, the kernel (18) only mildly diverges as $-R^{-1} \omega_c^2 \log|\tau|$, and if we would adopt the sharper cutoff $\text{Re} Y(\omega) = e^{-|\omega|/\omega_c}/R$, the kernel would even simply peak at $\pi\omega_c^2/4R + \mathcal{O}(\beta^{-2})$. With such more regular kernels, phase trajectories that vary more rapidly may contribute to the path integral, as well as paths ending in a well different from the initial one. This marked difference in paths that can contribute to the path integral qualitatively explains why our results may differ from those of WT.

Unfortunately, we cannot directly recover and check WT's results with our stochastic Liouville method because with the kernel (17), (i) $E_L = \frac{1}{2} \int_0^{\beta\hbar} d\tau K(\tau) = \infty$ and (ii) whatever the time discretization chosen, the strong K divergence at short times prevents drawing small stochastic increments for a proper numerical integration of the Liouville equation. Nevertheless, as shown above, in our approach we can investigate the limit of infinite environment cutoff numerically. This shows that a larger cutoff actually makes the junction more superconducting (something one cannot learn by considering from the onset an infinite cutoff). The observed trend at large cutoffs is actually simply explained by the counter-term localizing the phase more and more tightly (since $E_L \propto \omega_c$), which would ultimately yield a perfectly localized classical phase (and a superconducting

junction). Clearly, this trend with this limit are opposite of what would be needed to recover WT's result at infinite cutoff. We note, however, that these opposite results are obtained by taking limits differently : in our approach, we increase the cutoff to infinity after taking the low T limit of the path integral, while WT take the same limits in the reverse order. Baring errors in either numerical method, this indicates that these two limits do not commute. For a direct confirmation of this non-commutativity of limits one could use our finite-cutoff kernel in WT's quantum Monte-Carlo method. In that case, given the formal connection between the two methods, we expect the same results as ours would be obtained.

In summary, by choosing to use the kernel (17) in the action (16), one assumes (i) an infinite cutoff would correctly describe an actual RSJ experiment, and also supposes (ii) the environment cutoff can be taken to infinity before evaluating the path integral and considering its low temperature limit. The results obtained with our exact approach reveal that neither of these assumptions holds. In WT's work and in several others, the prediction of the insulating ground state for RSJs with $R > R_Q$ results from using this kernel (17) with its unfulfilled assumptions; this is sufficient to explain why this insulating state is not observed in experiments. More generally, in any actual RSJ experiment the dissipative bath has a finite UV cutoff [1] and our results show that taking into account the finiteness of this cutoff is required for correctly predicting the RSJ ground state, whatever the theoretical approach; it is not just a matter of taste or convenience (*e.g.* for the applicability of our stochastic Liouville method).

Beyond refuting the prediction of an insulating state in RSJs, the present work provides for the first time a reliable way of predicting the equilibrium behavior of JJs in presence of arbitrary linear environments –even frequency-dependent ones–, provided the impedance is not too small. In addition this technique can, in principle, be extended to address the dynamical response and out-of-equilibrium behavior of the JJ. In the opposite small shunting impedance regime, the approach should be doable in the dual picture, considering the coupling of the JJ charge with the impedance's fluctuating voltage.

6 Conclusions

Using an exact numerical method, we obtain the reduced density matrix and the expectation values of observables of a Josephson junction shunted by a resistance. Our approach recovers the CPB physics when the shunt resistor is made very large, as expected for a vanishing perturbation. The method can be extended to frequency-dependent environment impedances, and, in principle, also to dynamical situations.

Our results are compatible with all simple limits and all experimental observations on Josephson circuits. They notably capture the remarkable non-monotonic temperature dependence of the effective Josephson inductance observed in the experiment of Murani and coworkers. Our results fully support the conclusions of Murani and coworkers that a resistive shunt with $R > R_Q$ does not render a Josephson junction *insulating*. On the contrary, we find that a shunt resistance can only make a junction *more superconducting* than it would be in its absence.

Our results clearly differ from many works which predict an insulating ground state in the RSJ for $R > R_Q$ but with consistency problems in simple limits and, most importantly, not in agreement with JJ experiments. For at least some of these works, we show their prediction of an insulating state is due to considering from the onset an Ohmic environment with no UV cutoff.

Together with the experimental results of Ref. [15], this work should close decades of misunderstandings around Schmid's prediction applied to JJs, which raised mysterious paradoxes and controversies. In particular, one should no longer claim that JJs are becoming *insulating* in high impedance environments. Likewise, explanations for environment-related phenomena in JJ should no longer refer to Schmid's QPT in order to not create or maintain confusion regarding the physics at play.

7 Acknowledgments

We are grateful to H. Grabert, J. Stockburger, C. Ciuti, L. Giacomelli, F. Borletto, R. Riwar, N. Roch, X. Waintal, O. Maillet, S. Latil, C. Gorini and our colleagues of the Quantronics group at CEA-Saclay for stimulating discussions, comments and helpful inputs at various stages of this work initiated 6 years ago. This work is supported in part by ANR project Triangle ANR-20-CE47-0011-02.

Appendices

A On the interpretation of Schmid’s QPT in Josephson junctions

What Schmid saw as remarkable in his work [3], was the *localization effect* in one well at large enough friction. Indeed, at low friction, a delocalized particle is no surprise since one expects to recover Bloch states in the vanishing friction limit.

However, the way in which Schmid’s analogy was received by physicists familiar with the Josephson junction had a totally reversed “surprise factor” : The predicted localized JJ phase was seen as run-of-the-mill since it is just like the classical description of the JJ which the beginner first learns (although in this classical description, dissipation is not *needed* to have a superconducting device). On the contrary, the delocalized phase in the weak damping limit, which was the vanilla situation for Schmid’s original particle, was *interpreted* as an extraordinary situation in which the JJ would turn *insulating* under the action of the resistance, even when the corresponding friction force is vanishing. Indeed, according to what became the standard interpretation of Schmid’s analogy, *a JJ could only be superconducting when it experienced strong damping of its phase*, even if this was in contradiction with the classical understanding of the device and with already abundant experimental observations of supercurrents in unshunted, undamped, junctions (by far the easiest to make and measure). As a corollary, the situation where Schmid wisely considered the effects of dissipation should be marginal, quite unexpectedly turned into an fascinating fantasy, even though it meant abandoning the mere notion of a perturbative effect.

Unsurprisingly, early experiments attempting to assess the existence of the predicted “insulating state” always observed that large junctions (i.e. with $E_J \gg E_C$) current biased through a very large resistor were contradicting the prediction by remaining superconducting [32-34], with apparently no one ever pointing that it had always been so and had never seemed a problem before. For making these observations compatible with the above interpretation of Schmid’s analogy, the QPT prediction was patched, arguing that large undamped junctions were to be understood as being in a very long lived metastable superconducting state, with their “true insulating ground state” totally unreachable in practice [13, 34], while smaller junctions would actually reach their “insulating ground state”.

But even with this “metastability fix” for large junctions, the standard interpretation of Schmid’s prediction for JJ still had major consistency problems:

- First, Cooper-pair-box type of superconducting qubits with small unshunted junctions (i.e. the $R \rightarrow \infty$ limit of the RSJ) are found superconducting, contradicting both the prediction and the fix. This is obvious in the case where the junction is replaced by a squid: the observed temperature-independent flux tunability of such qubits implies that a dc supercurrent is circulating in the squid loop, so that neither of its junctions can actually be *insulating* (same argument as in Ref. [15]).
- Secondly, the standard interpretation of Schmid’s prediction also has a theoretical continuity problem in the limit of large-area junctions, where the anharmonicity of the qubit vanishes : there, the ground state behavior of an RSJ must come to match that of the parallel RLC circuit (with a linear superconducting inductor) whose ground state is superconducting because of the inductor, whatever the value of the shunt resistor.

To the best of our knowledge, the theoretical literature on Schmid's transition in Josephson junction has not properly discussed how the predicted insulating phase could be reconciled with the basic continuity expectations in these simple limits.

Given that the behavior of RSJs was already qualitatively very well known [35-37] long before the time of Schmid's prediction, it is hardly explainable in retrospect that the awkward consequences of the standard interpretation of Schmid's analogy were not immediately pointed as inconsistent with the established knowledge on JJs. It is even more surprising that for nearly forty years the community remained in a situation where it believed the standard interpretation of Schmid's QPT in JJs was indisputable, either ignoring the problems mentioned above, or not caring to resolve these oddities.

B Generation of discrete noise increments with required correlations

For the Lorentzian $\text{Re}Y(\omega)$ Eq. (2) we assume, the integral in (8) converges for $0 < \tau < \hbar\beta$ and admits the analytical solutions

$$\begin{aligned} S_{II}(-i\tau) &= \frac{\hbar}{\pi R} \omega_c^2 \left(\text{Re} \left[e^{-\frac{2i\pi\tau}{\beta\hbar}} \Phi \left(e^{-\frac{2i\pi\tau}{\beta\hbar}}, 1, \frac{\beta\hbar\omega_c}{2\pi} + 1 \right) \right] + \frac{\pi}{\beta\hbar\omega_c} \right) \\ &= \sum_{n=0}^{\infty} S_n \cos(\omega_n \tau) \end{aligned} \quad (18)$$

where Φ is the Lerch transcendent function, and $S_n = \frac{\hbar}{R} \omega_c^2 \frac{(2 - \delta_{n0})}{\beta\hbar\omega_c + 2\pi n}$, $\omega_n = n \frac{2\pi}{\beta\hbar}$. These last two expressions are even and $\hbar\beta$ -periodic in τ (and, of course, symmetric about $\tau = \hbar\beta/2$). At $\tau \sim 0$ these expressions have a mild divergence $S_{II}(-i\tau) \sim R^{-1} \omega_c^2 \log|\tau|$ (See Fig. 4). Other forms of $\text{Re}Y(\omega)$ with a sharper cutoff, such as e.g. $\text{Re}Y(\omega) = \exp(-|\omega|/\omega_c)/R$, are even free of divergence.

For satisfying Eq. (9), the random noise $\xi(\tau_n)$ can be naively drawn as the real numbers

$$\xi(\tau_n) = \sum_{m=0}^{M-1} R_m \cos(\omega_m \tau_n + \theta_m) \quad (19)$$

where $\theta_0 = \pi/2$, R_0 is random number normally-distributed with zero mean and variance $2S_0$, and the $\{R_{m>0}\}$ are taken fixed as $R_{m>0} = \sqrt{2S_m}$, with the $\{\theta_{m>0}\}$ random and uniformly-distributed in $[0, 2\pi[$. Then, the $\{\xi(\tau_n)\}$ ensemble (Eq. (19)) is efficiently obtained as the real part of the fast Fourier transform (FFT) of $\{e^{i\theta_m} R_m\}$. With this construction, the correlators are

$$\begin{aligned} \langle \xi(\tau_n) \xi(\tau_m) \rangle &= \sum_{j,k=0}^{M-1} \langle R_k R_j \cos(\omega_k \tau_n + \theta_k) \cos(\omega_j \tau_m + \theta_j) \rangle \\ &= \sum_{j,k=0}^{M-1} \frac{1}{2} \{ \langle R_k R_j \cos(\delta\tau \delta\omega (j m - k n) - \theta_k + \theta_j) \rangle \\ &\quad + \langle R_k R_j \cos(\delta\tau \delta\omega (k n + j m) + \theta_k + \theta_j) \rangle \} \\ &= \langle R_0^2 \rangle \frac{1}{2} + \sum_{j=1}^{M-1} R_j^2 \frac{1}{2} (\cos(\delta\tau \delta\omega j(m-n))) + \langle R_0^2 \rangle \frac{1}{2} \cos(2\theta_0) \\ &= \sum_{j=0}^{M-1} S_j \cos(j(m-n)\delta\tau\delta\omega) \\ &= S_{II}(-i(\tau_n - \tau_m)) - \sum_{j=M}^{\infty} S_j \cos(j(m-n)\delta\tau\delta\omega) \end{aligned} \quad (20)$$

which apparently almost fits the requirement (Eq. (9)).

The first problem with this naive algorithm is the logarithmic divergence of $S_{II}(-i\tau)$ at $\tau=0$, for the Lorentzian $\text{Re} Y(\omega)$ we consider. This is solved by taking, instead of $S_{II}(-i(\tau_n))$, the averaged $\bar{S}_{II}(-i(\tau_n)) = \delta\tau^{-1} \int_{\tau_n - \delta\tau/2}^{\tau_n + \delta\tau/2} S_{II}(-i\tau) d\tau$ over the time steps of our discretization, which removes the weak divergence. This amounts to filtering the correlation function by convolving it by a rectangular function, and hence to multiply the Fourier coefficients S_n by a sinc

$$S_n \rightarrow \bar{S}_n = S_n \text{sinc} \frac{\delta\tau}{2} \omega_n = S_n \text{sinc} \frac{n\pi}{M},$$

and to define the $\{R_m\}$ from these $\{\bar{S}_m\}$.

Even with such filtering, a second problem remains : when taking the FFT, we only sum the M first Fourier coefficients so that the correlator we obtain deviates from the ideal value, as apparent in Eq. (20). When M is large enough, this deviation leaves a noticeable systematic error only for the same-time correlator

$$\langle \xi(\tau_n) \xi(\tau_n) \rangle = \bar{S}_{II}(0) - \Delta$$

where the error Δ is

$$\Delta = \sum_{j=M}^{\infty} \bar{S}_j = \frac{\hbar}{R} \omega_c^2 \frac{M \text{Im} \left(\Phi \left(e^{-\frac{i\pi}{M}}, 1, M \right) - \Phi \left(e^{-\frac{i\pi}{M}}, 1, M + \frac{\beta \hbar \omega_c}{2\pi} \right) \right)}{\pi \beta \hbar \omega_c}.$$

Such Dirac delta-like error can be easily corrected by applying a shift to all the Fourier coefficients entering our FFT, except the zero-frequency one which provides the correct baseline

$$\bar{S}_j \rightarrow \tilde{S}_j = \bar{S}_j - (1 - \delta_{0j}) \frac{\Delta}{M - 1}, \quad j = 0, \dots, M - 1.$$

The $\{R_m\}$ are finally evaluated from the $\{\tilde{S}_m\}$ in place of the initial $\{S_m\}$. With these corrections made, we compare the numerical correlations to the expected $\bar{S}_{II}(-i(\tau))$ in Fig. 4

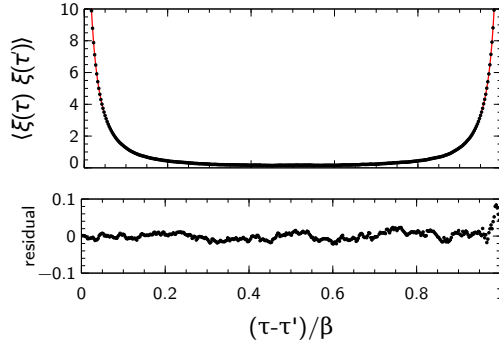


Figure 4. Comparison of the filtered (see text) theoretical current noise correlator in imaginary time for a Lorentzian $\text{Re} Y(\omega)$ (red continuous line) and experimental correlator for 10^6 drawings of a noise sequence (black dots). The bottom panel shows the difference between the numerical correlator and its expected value. Parameters are $R = 3R_Q$, $\beta\hbar\omega_c = 30$, 401 time steps.

C Basis states, operator matrices and thermal expectation values for the bare CPB

In this appendix we evaluate thermal expectations values of some operators of the CPB, working in the eigenbasis. The CPB eigenstates can easily be obtained numerically in a truncated discrete charge basis, but below we rather obtain them analytically in terms of Mathieu functions [38, 39].

The Shrödinger differential equation for the bare CPB Hamiltonian is

$$E_C \Psi''(\varphi) - (E_J \cos \varphi) \Psi(\varphi) = E \Psi(\varphi). \quad (21)$$

which is a form of Mathieu's equation

$$f''(z) + (a - 2q \cos 2z) f(z) = 0$$

whose solutions are known as special functions [40]. Furthermore, given that the potential is periodic in φ , Bloch's theorem implies the eigenfunctions are of the form

$$\Psi_{np}(\varphi) = \langle \varphi | n, p \rangle = e^{ip\varphi} u_{np}(\varphi)$$

where n is a band index, and $p \in [-0.5, 0.5]$ is the quasicharge (i.e. Bloch's quasimomentum) in the first Brillouin zone (FBZ), with $u_{np}(\varphi)$ a 2π -periodic function (same period as the $\cos \varphi$ potential). If the CPB is not connected to anything, p is fixed to zero (a non-zero offset charge imposed by the surrounding is not taken into account in (21) but it could be simply added), whereas when connected to a circuit that can let charge circulate, p can fluctuate and take any value.

Using knowledge from the solutions of Mathieu's equation, the eigenenergy E_{np} of $\Psi_{np}(\varphi)$ is given by

$$E_{np} = \frac{E_C}{4} \lambda_{\chi(n,p)}(-2E_J/E_C)$$

where λ_ν denotes the Mathieu characteristic value indexed by its so-called characteristic exponent and

$$\chi(n, p) = n + n \bmod 2 + (-1)^n 2|p|$$

is a function giving the characteristic exponents in the FBZ such that the eigenenergies are sorted increasing with the band index $n \geq 0$. The u_{np} functions themselves are given by

$$u_{np}(\varphi) = \frac{e^{-ip\varphi}}{\sqrt{2\pi}} \left(\text{ce}_{\chi(n,p)} \left(\frac{\varphi}{2}, -2 \frac{E_J}{E_C} \right) + i (-1)^n \text{sign}(p) \text{se}_{\chi(n,p)} \left(\frac{\varphi}{2}, -2 \frac{E_J}{E_C} \right) \right)$$

where ce_ν and se_ν are respectively even and odd real functions of φ [40]. Note that λ_ν has discontinuities when $\nu = \chi(n, p)$ is strictly an integer (i.e. when $|p| = 0$ or $1/2$ in the FBZ), as well as either ce_ν or se_ν ; the eigensolutions to consider at these values in each band are then obtained as the limits when approaching the discontinuity. Note also that our expressions resemble but are not mathematically identical to previously published forms [38, 39].

It is then straightforward to obtain the matrix elements of $N = -i \frac{\partial}{\partial \varphi}$ and N^2 :

$$\begin{aligned} \langle n, p | N | n', p' \rangle &= \delta(p - p') \left(\delta_{nn'} p - i \int_0^{2\pi} d\varphi u_{np}^*(\varphi) \frac{d u_{n'p}(\varphi)}{d\varphi} \right), \\ \langle n, p | N^2 | n', p' \rangle &= \delta(p - p') \left(\delta_{nn'} p^2 - 2i p \int_0^{2\pi} d\varphi u_{np}^*(\varphi) \frac{d u_{n'p}(\varphi)}{d\varphi} \right. \\ &\quad \left. - \int_0^{2\pi} d\varphi u_{np}^*(\varphi) \frac{d^2 u_{n'p}(\varphi)}{d\varphi^2} \right), \\ &= \delta(p - p') \left(\delta_{nn'} p^2 - 2i p \int_0^{2\pi} d\varphi u_{np}^*(\varphi) \frac{d u_{n'p}(\varphi)}{d\varphi} \right. \\ &\quad \left. + \int_0^{2\pi} d\varphi \frac{d u_{np}^*(\varphi)}{d\varphi} \frac{d u_{n'p}(\varphi)}{d\varphi} \right), \end{aligned}$$

and those of any function $f(\varphi)$ are

$$\langle n, p | f(\varphi) | n', p' \rangle = \delta(p - p') \int_0^{2\pi} d\varphi f(\varphi) u_{np}^*(\varphi) u_{n'p}(\varphi),$$

Finally, we can evaluate thermal equilibrium expectation values from the thermal density matrix $\rho_\beta = e^{-\beta H} / \text{Tr} e^{-\beta H}$ and the matrix elements of operators as

$$\langle A \rangle = \text{Tr} \rho_\beta A = \sum_n \int_{-1/2}^{1/2} dp e^{-\beta E_{np}} \langle n, p | A | n, p \rangle$$

In qubits, the quasicharge charge p has values externally imposed by the gate. The low impedance of the gate voltage is such that p is nearly fixed and one should then only sum over the band index. In Fig. 5, assuming either fixed charge offset or that p (or n_g) can take any value, we plot the thermal expectation values $\sigma_N = \langle N^2 \rangle^{1/2}$ of the rms fluctuations of the charge N , and the Josephson coherence factor $\langle \cos \varphi \rangle$, which are both indicators of the superconducting character of the CPB. Indeed, if the junction were insulating, N could not fluctuate at all and its effective inductance $L_{\text{eff}} = \varphi_0^2 / E_J \langle \cos \varphi \rangle$ would be infinite ($\langle \cos \varphi \rangle$ vanishes). One could also consider $\langle \sin^2 \varphi \rangle$, the fluctuations of the supercurrent: if they are non-zero the junction cannot be insulating. However a vanishing of $\langle \sin^2 \varphi \rangle$ is ambiguous since $\langle \sin^2 \varphi \rangle = 0$ both for an insulating junction and the classical superconducting junction in absence of phase bias.

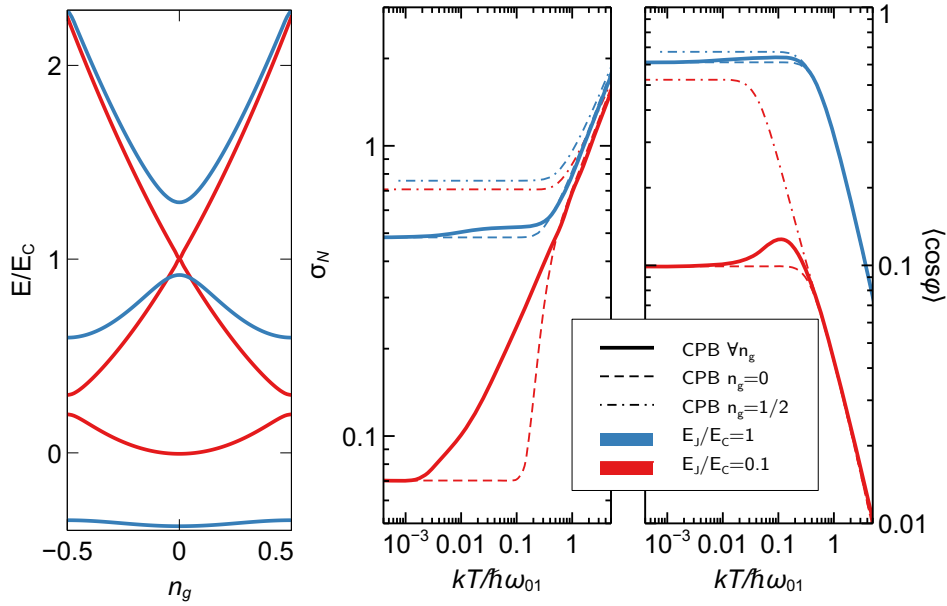


Figure 5. For all panels, red: $E_J = 0.1E_C$, blue: $E_J = E_C$ and $\hbar\omega_{01} = E_1(n_g=0) - E_0(n_g=0)$. Left panel: energy bands E_0 , E_1 and E_2 (from bottom to top) of the CPB as a function of the gate charge. Middle (resp. right) panel, thermal expectation values of rms fluctuations of the charge N (resp. Josephson coherence factor $\langle \cos \varphi \rangle$) as a function of temperature, for fixed gate charge $n_g=0$ (thin dashed lines), $n_g=1/2$ (thin dashed-dot lines), or (thick full lines) when allowing all gate charges.

This figure shows that at high temperatures, when $kT \gtrsim \hbar\omega_{01}$ (temperature larger than the separation of the first two bands at $n_g=0$), the expectation values follow power laws $\sigma_N \propto T^{1/2}$ and $\langle \cos \varphi \rangle \propto T^{-1}$, with values independent of whether n_g is kept fixed or allowed to vary. In the opposite low temperature limit where $kT \ll E_0(n_g=1/2) - E_0(n_g=0)$ (the amplitude of the ground quasicharge band), expectation values saturate to a plateau corresponding to the zero point fluctuations of the ground state at $n_g=0$.

In the intermediate temperature range, allowing charge fluctuations on the capacitor enhances both σ_N and $\langle \cos \varphi \rangle$ with respect to the fixed $n_g=0$ case, and this effect is most pronounced when E_C/E_J is large (deep ground quasicharge band). For $\langle \cos \varphi \rangle$, this notably leads to a striking non-

monotonous T – dependence, with a local maximum at $kT \sim 0.1\hbar\omega_{01}$. This maximum is easily explained. In JJs with $E_C \gg E_J$, Cooper pair transfer occurs mostly through a second order tunneling process of quasiparticles, with a virtual intermediate state on higher charge parabolas. When allowing thermal fluctuations of the quasicharge away from 0 in the ground band, the energy difference between the ground and the lowest virtual excited state is reduced, hence increasing the effective Josephson coupling. At temperatures $kT \sim \hbar\omega_{01}$ or higher, the excited bands also get populated which then reduces the effective Josephson coupling.

D About recent reaffirmations of the existence of Schmid’s dissipative QPT in JJs.

In this appendix, we discuss some recently published works on JJs, all claiming to confirm the existence of the Schmid QPT in JJs (possibly in some reduced parameter range).

In the experimental Ref. [20] the authors conclude to the existence of a the Schmid “insulating state” based on the measurement of a SQUID modulation which, curiously, is the exact same argument used in Ref. [15] to conclude to the absence of an insulating state (see above, in the Introduction). Regrettably, that work does not report any T -power law of their measurements which would rigorously prove their experiment is in a quantum critical regime.

In the theoretical Ref. [21], the authors examine the microwave reflection on a Josephson junction connected to a semi-infinite transmission line with a characteristic impedance R for implementing the shunt resistance of the RSJ. Indeed, the authors find a phaseshift of a reflected signal when R varies, very similar to what was observed in the work just discussed [20]. For obtaining their results the authors assume that in the $R \rightarrow \infty$ limit one must recover the physics of the bare CPB results (and we fully agree), and they use this limit to evaluate the phaseshift. Although the authors evoke the vanishing of the effective Josephson coupling due to the Schmid QPT in their conclusions, such vanishing does not occur in the bare CPB limit on which their work is based. What the authors actually show is that the experimental results of Ref. [20] can be interpreted without the junction becoming insulating, making the results of those works compatible with the conclusions of the present work and of Ref. [15]. The above change in reflection phaseshift could perhaps qualify as a QPT of some type, but in which the junction would definitely not be insulating in either phase.

Finally, the works in Refs. [18, 19, 41] are based on renormalization group (RG) techniques and confirm the existence of a QPT at least in a partial parameter range. Yet, they disagree on the phase boundary, exposing how tricky it can be to obtain reliable RG results for that system. We suspect these works predict a QPT for the same reason as Werner and Troyer [12] (see Sec. 5), i.e. not properly taking into account the UV cutoff in the environment admittance.

Bibliography

- [1] A. O. Caldeira and A. J. Leggett, *Quantum tunnelling in a dissipative system*, Annals of Physics **149**(2), 374 (1983), doi:10.1016/0003-4916(83)90202-6.
- [2] M. H. Devoret, J. M. Martinis and J. Clarke, *Measurements of Macroscopic Quantum Tunneling out of the Zero-Voltage State of a Current-Biased Josephson Junction*, Physical Review Letters **55**(18), 1908 (1985), doi:10.1103/PhysRevLett.55.1908.
- [3] A. Schmid, *Diffusion and Localization in a Dissipative Quantum System*, Physical Review Letters **51**(17), 1506 (1983), doi:10.1103/PhysRevLett.51.1506.
- [4] H. Kohler, F. Guinea and F. Sols, *Quantum electrodynamic fluctuations of the macroscopic Josephson phase*, Annals of Physics **310**(1), 127 (2004), doi:10.1016/j.aop.2003.08.014.
- [5] N. Kimura and T. Kato, *Temperature dependence of zero-bias resistances of a single resistance-shunted Josephson junction*, Physical Review B **69**(1), 012504 (2004), doi:10.1103/PhysRevB.69.012504.
- [6] C. P. Herrero and A. D. Zaikin, *Superconductor-insulator quantum phase transition in a single Josephson junction*, Physical Review B **65**(10), 104516 (2002), doi:10.1103/PhysRevB.65.104516.
- [7] G.-L. Ingold and H. Grabert, *Effect of Zero Point Phase Fluctuations on Josephson Tunneling*, Physical Review Letters **83**(18), 3721 (1999), doi:10.1103/PhysRevLett.83.3721.
- [8] A. D. Zaikin and S. V. Panyukov, *Dynamics of a quantum dissipative system: Duality between coordinate and quasimomentum spaces*, Physics Letters A **120**(6), 306 (1987), doi:10.1016/0375-9601(87)90677-3.
- [9] C. Aslangul, N. Pottier and D. Saint-James, *Quantum ohmic dissipation: Particle on a one-dimensional periodic lattice*, Physics Letters A **111**(4), 175 (1985), doi:10.1016/0375-9601(85)90570-5.
- [10] F. Guinea, V. Hakim and A. Muramatsu, *Diffusion and Localization of a Particle in a Periodic Potential Coupled to a Dissipative Environment*, Physical Review Letters **54**(4), 263 (1985), doi:10.1103/PhysRevLett.54.263.

- [11] S. L. Lukyanov and P. Werner, *Resistively shunted Josephson junctions: Quantum field theory predictions versus Monte Carlo results*, Journal of Statistical Mechanics: Theory and Experiment **2007**(06), P06002 (2007), doi:10.1088/1742-5468/2007/06/P06002.
- [12] P. Werner and M. Troyer, *Efficient Simulation of Resistively Shunted Josephson Junctions*, Physical Review Letters **95**(6), 060201 (2005), doi:10.1103/PhysRevLett.95.060201.
- [13] G. Schön and A. D. Zaikin, *Quantum coherent effects, phase transitions, and the dissipative dynamics of ultra small tunnel junctions*, Physics Reports **198**(5-6), 237 (1990), doi:10.1016/0370-1573(90)90156-V.
- [14] E. D. Torre and E. Sela, *Viewpoint: Circuit Simulates One-Dimensional Quantum System*, Physics **11** (2018), doi:10.1103/Physics.11.94.
- [15] A. Murani, N. Bourlet, H. le Sueur, F. Portier, C. Altimiras, D. Esteve, H. Grabert, J. Stockburger, J. Ankerhold and P. Joyez, *Absence of a Dissipative Quantum Phase Transition in Josephson Junctions*, Physical Review X **10**(2), 021003 (2020), doi:10.1103/PhysRevX.10.021003.
- [16] M. Vojta, *Quantum phase transitions*, Reports on Progress in Physics **66**(12), 2069 (2003), doi:10.1088/0034-4885/66/12/R01.
- [17] T. Morel and C. Mora, *Double-periodic Josephson junctions in a quantum dissipative environment*, Physical Review B **104**(24), 245417 (2021), doi:10.1103/PhysRevB.104.245417.
- [18] R. Daviet and N. Dupuis, *On the nature of the superconductor-insulator transition in a resistively shunted Josephson junction*.
- [19] K. Masuki, H. Sudo, M. Oshikawa and Y. Ashida, *Absence versus Presence of Dissipative Quantum Phase Transition in Josephson Junctions*, Physical Review Letters **129**(8), 087001 (2022), doi:10.1103/PhysRevLett.129.087001.
- [20] R. Kuzmin, N. Mehta, N. Grabon, R. A. Mencia, A. Burshtein, M. Goldstein and V. E. Manucharyan, *Observation of the Schmid-Bulgadaev dissipative quantum phase transition*, doi:10.48550/arXiv.2304.05806 (2023), 2304.05806.
- [21] M. Houzet, T. Yamamoto and L. I. Glazman, *Microwave spectroscopy of Schmid transition*, doi:10.48550/arXiv.2308.16072 (2023), 2308.16072.
- [22] V. E. Manucharyan, J. Koch, L. I. Glazman and M. H. Devoret, *Fluxonium: Single Cooper-Pair Circuit Free of Charge Offsets*, Science **326**(5949), 113 (2009), doi:10.1126/science.1175552.
- [23] J. Koch, V. Manucharyan, M. H. Devoret and L. I. Glazman, *Charging Effects in the Inductively Shunted Josephson Junction*, Physical Review Letters **103**(21), 217004 (2009), doi:10.1103/PhysRevLett.103.217004.
- [24] H. Grabert, P. Schramm and G.-L. Ingold, *Quantum Brownian motion: The functional integral approach*, Physics Reports **168**(3), 115 (1988), doi:10.1016/0370-1573(88)90023-3.
- [25] *Quantum Dissipative Systems*, vol. 13 of *Series in Modern Condensed Matter Physics*, WORLD SCIENTIFIC, Singapore, 3 edn., ISBN 978-981-279-162-7 978-981-279-179-5 (2008).
- [26] R. P. Feynman and F. L. Vernon, *The theory of a general quantum system interacting with a linear dissipative system*, Annals of Physics **24**, 118 (1963), doi:10.1016/0003-4916(63)90068-X.
- [27] J. M. Moix, Y. Zhao and J. Cao, *Equilibrium-reduced density matrix formulation: Influence of noise, disorder, and temperature on localization in excitonic systems*, Physical Review B **85**(11), 115412 (2012), doi:10.1103/PhysRevB.85.115412.
- [28] G. M. G. McCaul, C. D. Lorenz and L. Kantorovich, *Partition-free approach to open quantum systems in harmonic environments: An exact stochastic Liouville equation*, Physical Review B **95**(12), 125124 (2017), doi:10.1103/PhysRevB.95.125124.
- [29] J. T. Stockburger and H. Grabert, *Exact c-Number Representation of Non-Markovian Quantum Dissipation*, Physical Review Letters **88**(17), 170407 (2002), doi:10.1103/PhysRevLett.88.170407.
- [30] M. Riesch and C. Jirauschek, *Analyzing the positivity preservation of numerical methods for the Liouville-Neumann equation*, Journal of Computational Physics **390**, 290 (2019), doi:10.1016/j.jcp.2019.04.006.
- [31] P. Joyez, *Self-Consistent Dynamics of a Josephson Junction in the Presence of an Arbitrary Environment*, Physical Review Letters **110**(21), 217003 (2013), doi:10.1103/PhysRevLett.110.217003.
- [32] L. S. Kuzmin, Yu. V. Nazarov, D. B. Haviland, P. Delsing and T. Claeson, *Coulomb blockade and incoherent tunneling of Cooper pairs in ultrasmall junctions affected by strong quantum fluctuations*, Physical Review Letters **67**(9), 1161 (1991), doi:10.1103/PhysRevLett.67.1161.
- [33] R. Yagi, S.-i. Kobayashi and Y. Ootuka, *Phase Diagram for Superconductor-Insulator Transition in Single Small Josephson Junctions with Shunt Resistor*, Journal of the Physical Society of Japan **66**(12), 3722 (1997), doi:10.1143/JPSJ.66.3722.
- [34] J. S. Penttilä, Ü. Parts, P. J. Hakonen, M. A. Paalanen and E. B. Sonin, *“Superconductor-Insulator Transition” in a Single Josephson Junction*, Physical Review Letters **82**(5), 1004 (1999), doi:10.1103/PhysRevLett.82.1004.
- [35] D. E. McCumber, *Effect of ac Impedance on dc Voltage-Current Characteristics of Superconductor Weak-Link Junctions*, Journal of Applied Physics **39**, 3113 (1968), doi:10.1063/1.1656743.
- [36] W. C. Stewart, *Current-Voltage Characteristics of Josephson Junctions*, Applied Physics Letters **12**, 277 (1968), doi:10.1063/1.1651991.
- [37] Yu. M. Ivanchenko and L. A. Zil’berman, *The Josephson Effect in Small Tunnel Contacts*, Soviet Journal of Experimental and Theoretical Physics **28**, 1272 (1969).
- [38] J. Koch, T. M. Yu, J. Gambetta, A. A. Houck, D. I. Schuster, J. Majer, A. Blais, M. H. Devoret, S. M. Girvin and R. J. Schoelkopf, *Charge insensitive qubit design derived from the Cooper pair box*, Physical Review A **76**(4), 042319 (2007), doi:10.1103/PhysRevA.76.042319, cond-mat/0703002.

- [39] A. Cottet, *Implémentation d'un bit quantique dans un circuit supraconducteur / Implementation of a quantum bit in a superconducting circuit*, Ph.D. thesis, Université Pierre et Marie Curie - Paris VI (2002).
- [40] *NIST digital library of mathematical functions: 28.12 Mathieu Functions of Noninteger Order*, <https://dlmf.nist.gov/28.12>.
- [41] T. Sépulcre, S. Florens and I. Snyman, *Comment on "Absence versus Presence of Dissipative Quantum Phase Transition in Josephson Junctions"*, doi:10.48550/arXiv.2210.00742 (2022), 2210.00742.